

Role of cytoplasmic dynein in the axonal transport of microtubules and neurofilaments

Yan He,¹ Franto Francis,² Kenneth A. Myers,¹ Wenqian Yu,¹ Mark M. Black,² and Peter W. Baas¹

¹Department of Neurobiology and Anatomy, Drexel University College of Medicine, Philadelphia, PA 19129

²Department of Anatomy and Cell Biology, Temple University School of Medicine, Philadelphia, PA 19140

Recent studies have shown that the transport of microtubules (MTs) and neurofilaments (NFs) within the axon is rapid, infrequent, asynchronous, and bidirectional. Here, we used RNA interference to investigate the role of cytoplasmic dynein in powering these transport events. To reveal transport of MTs and NFs, we expressed EGFP-tagged tubulin or NF proteins in cultured rat sympathetic neurons and performed live-cell imaging

of the fluorescent cytoskeletal elements in photobleached regions of the axon. The occurrence of anterograde MT and retrograde NF movements was significantly diminished in neurons that had been depleted of dynein heavy chain, whereas the occurrence of retrograde MT and anterograde NF movements was unaffected. These results support a cargo model for NF transport and a sliding filament model for MT transport.

Introduction

Early studies on slow axonal transport suggested that the proteins that comprise microtubules (MTs), actin filaments, and neurofilaments (NFs) are transported in the form of assembled polymers (Black and Lasek, 1980). Photobleach studies performed in the 1990s failed to reveal coherent movement of the polymers, leading to the theory that the polymers are stationary, whereas the proteins move in an unassembled form (Lim et al., 1990). Using longer bleached zones and natural gaps in the NF array, it has been observed in more recent studies that MTs and NFs are indeed in motion, but move rapidly, asynchronously, bidirectionally, and intermittently (Wang et al., 2000; Roy et al., 2000; Wang and Brown, 2001, 2002). These observations suggest that slow axonal transport is a collection of fast but infrequent movements, which appear slow when the population of moving and nonmoving polymers are studied collectively. Cytoplasmic dynein is a good candidate as a motor for slow axonal transport because it generates a variety of cytoskeletal movements in other cell types (Abal et al., 2002; Dujardin et al., 2003).

Cytoplasmic dynein moves toward minus ends of MTs, and thereby transports vesicular organelles in the retrograde direction in the axon. In a “cargo” model for slow axonal transport, cytoplasmic dynein would also convey short MTs and NFs retrogradely by moving them along longer MTs. If this is correct, then the anterograde movements are presumably generated by members of the kinesin superfamily. Alternatively, in a

“sliding filament” model, cytoplasmic dynein could fuel anterograde transport of short MTs if the cargo domain of dynein interfaces with a structure with more resistance to movement than the short MT (Ahmad et al., 1998). In the classic radiolabel paradigm for slow axonal transport, cytoplasmic dynein tends to move at the somewhat faster rate of actin filaments rather than the somewhat slower rate of MTs and NFs (Dillman et al., 1996). On this basis, it was proposed that the cargo-binding domain of the motor interfaces with the actin cytoskeleton, leaving the motor domain available to translocate MTs. It is also possible that bidirectional MT movements occur along other MTs, with the directionality depending on the configuration of the motor between the moving and nonmoving MT. Such movements could be fueled entirely by cytoplasmic dynein or might involve other motors as well. The sliding filament model might also account for NF transport, if the NFs simply “piggy back” on MTs through nonmotor cross-links, and move as the MT moves (Brady, 2000).

Understanding the specific roles of cytoplasmic dynein in MT and NF transport is key to distinguishing between the cargo model and the sliding filament model for each cytoskeletal element, and hence for elucidating the mechanisms that orchestrate slow axonal transport.

Results and discussion

Diminution of dynein heavy chain (DHC) in cultured sympathetic neurons by siRNA

We used a mixture of four different siRNA duplexes that target different regions on the mRNA of DHC. Quantitative immuno-

Correspondence to P.W. Baas: Peter.W.Baas@drexel.edu

Abbreviations used in this paper: DHC, dynein heavy chain; MT, microtubule; NF, neurofilament.

The online version of this article includes supplemental material.

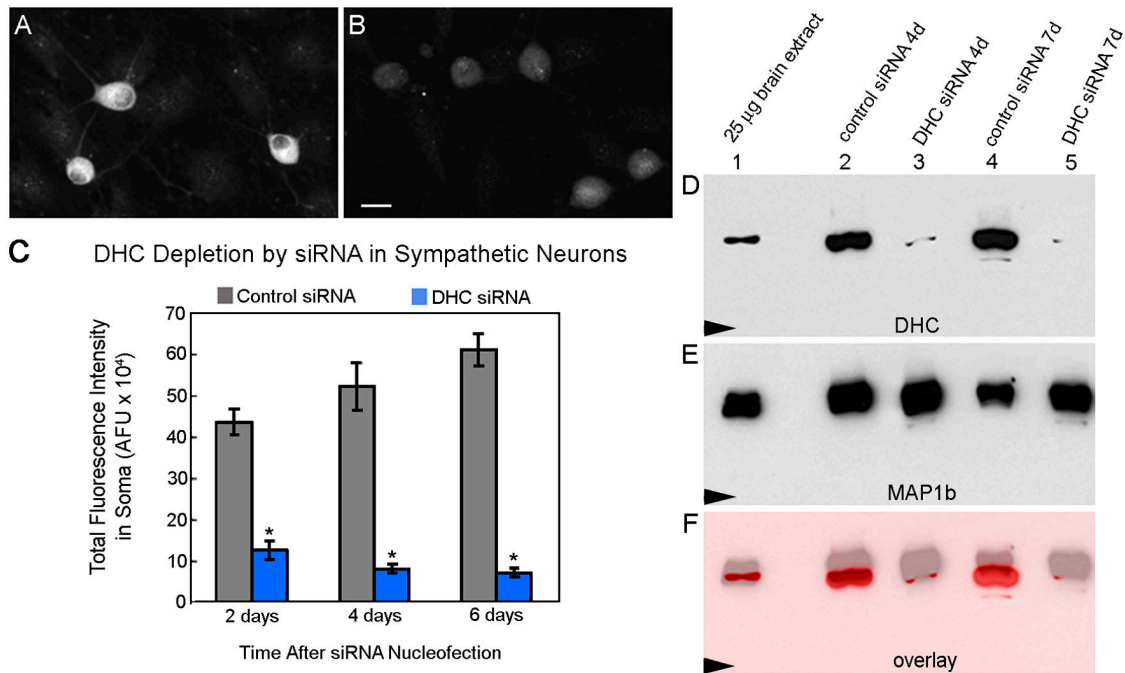


Figure 1. **Depletion of DHC by siRNA.** Immunofluorescence indicates depletion of DHC in DHC siRNA-treated sympathetic neurons (B), compared with control siRNA-treated neurons (A). (C) Quantification of total fluorescent intensity within soma revealed the progression of DHC depletion by siRNA (*t*-test, *, $P < 0.05$). Western blots of whole cell extracts probed with the DHC antibody (D) confirmed the protein lowering effect. The blot was stripped and reprobed with a MAP1b antibody (E), and the overlay (F) confirmed the specificity of both the DHC antibody and the DHC depletion by siRNA. Arrowheads in D–F indicate the 219-kD molecular mass marker. Bar, 20 μm .

fluorescence images revealed that more than 80% of neurons in DHC siRNA-treated cultures exhibit a dramatic diminution of the protein (Fig. 1, A and B). Significant protein reduction starts as early as 2 d and proceeds at least until 6 d after siRNA transfection when <20% of the protein is still present (Fig. 1 C). Western blot analyses confirmed the drastic depletion of DHC by siRNA (Fig. 1 D). Furthermore, when stripped and reprobed with a MAP1b antibody, the DHC bands migrated just ahead of the MAP1b bands, as expected (Bloom et al., 1984), and we detected no diminution in the levels of MAP1b as a result of the DHC siRNA (Fig. 1, E and F). Therefore, assuming that the DHC antibody recognizes most or all isoforms of the DHC protein, we are able to specifically knock down at least 80% and perhaps over 90% of the protein in sympathetic neurons.

In a previous paper, we reported that acute disruption of dynein by microinjection of recombinant dynamitin impairs both axonal growth and MT transport from the neuronal centrosome (Ahmad et al., 1998). We used the siRNA approach for the present work because dynein disruption is now known to have effects in addition to dynein inhibition (Schroer, 2004). Unlike acute dynein disruption, the gradual depletion of DHC by siRNA did not markedly impair the formation and growth of axons. These differing results may relate to the broader effects of dynein disruption and/or to the longer period of time required for the cessation of dynein function with the siRNA approach.

Golgi disruption and interruption of vesicle traffic by DHC depletion

Golgi dispersion is a reliable indicator of dynein inhibition. In control siRNA-treated neurons, the Golgi apparatus appears as

a compact, multi-tubule structure located near the cell center (Fig. 2 A). In DHC-depleted neurons, the Golgi apparatus became elongated, less compact, and distributed throughout the cell body after 4 d of siRNA treatment (Fig. 2 B). Quantification of Golgi size revealed that the dispersion became significant from 4 d and progressed until 6 d after siRNA transfection (Fig. 2 C). We also examined vesicle transport behaviors in living sympathetic neurons treated with control or DHC siRNA. Neurons were incubated with rhodamine-dextran to label a subfraction of vesicular structures arising from endocytosis (Hollenbeck, 1993). The moving behaviors of fluorescent vesicles were recorded by time-lapse imaging and analyzed for both the frequency and the persistence of their movements within the axon. We found that by 2 d after transfection, the number of anterogradely and retrogradely moving vesicles per axon per minute was not affected by DHC siRNA treatment (*t*-test; Fig. 2 E and Table S1, available at <http://www.jcb.org/cgi/content/full/jcb.200407191/DC1>). In addition, the percentage of vesicles that exhibit processive or sustained motion (for definition see Materials and methods; Fig. 2 D) was not affected in either direction at 2 d of DHC siRNA treatment (*t*-test; Fig. 2 E and Table S1). However, by 4 d after DHC siRNA transfection, the frequencies of vesicle movements were significantly diminished in both anterograde and retrograde directions, and to similar extent (Fig. 2 E and Table S1). The percentage of sustained movements was decreased, but not significantly, in the anterograde direction (13% decrease; $P = 0.07$). However, the percentage of labeled vesicles exhibiting sustained retrograde movements was significantly decreased by DHC depletion (43% decrease; $P = 0.01$; Fig. 2 E and Table S1).

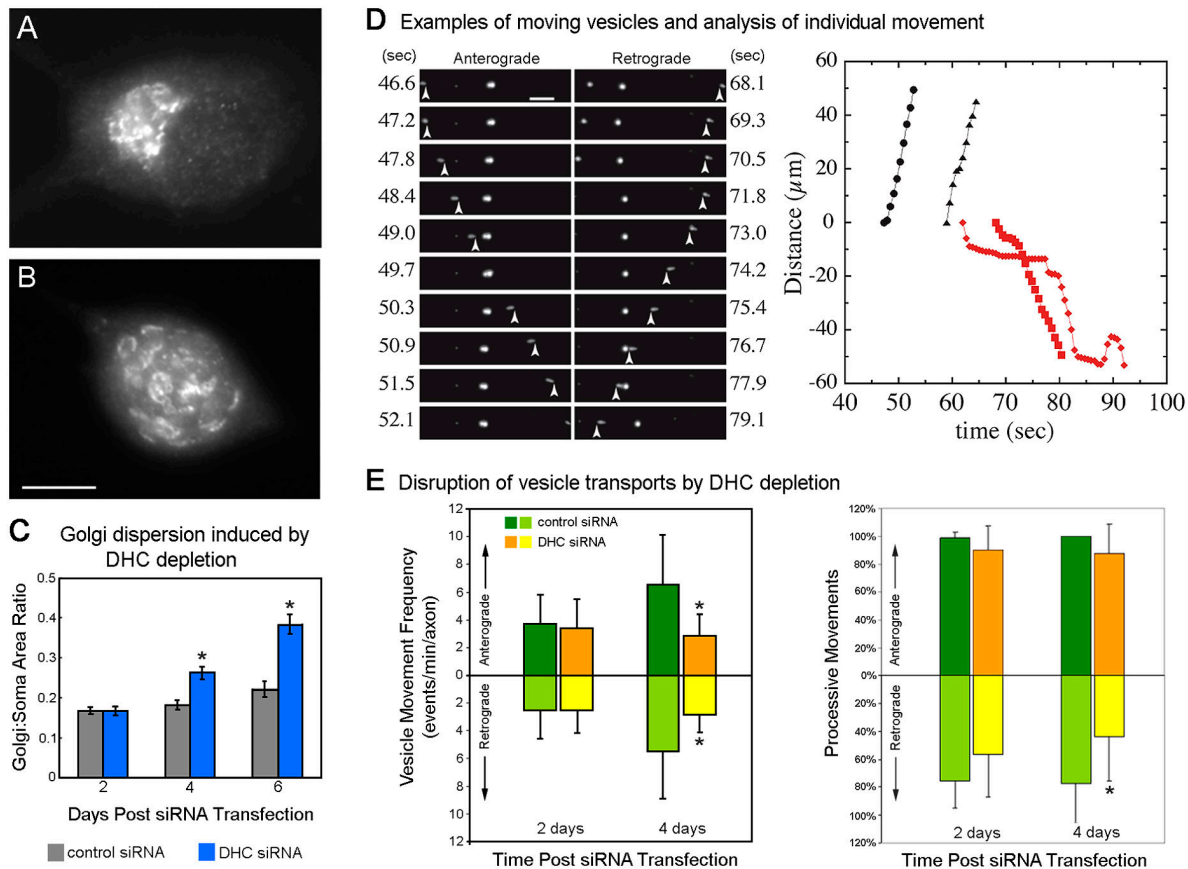


Figure 2. DHC depletion results in Golgi dispersion and partial vesicle transport inhibition. Golgi-58K protein immunostaining revealed compact Golgi apparatus in a control siRNA-treated neuron (A) and dispersed Golgi apparatus in a DHC siRNA-treated neuron (B) 6 d after siRNA transfection. (C) Quantification of Golgi area relative to soma area revealed a gradual increase of the Golgi size in DHC siRNA-treated neurons (#test, *, $P < 0.05$) starting from 4 d after siRNA transfection. Bar, 10 μm . (D) Left panel shows an anterogradely moving vesicle (arrowhead) with elapsed time in seconds. Distance traversed is depicted by closed circles in graph. Right panel shows a retrogradely transported vesicle (arrowhead), with movement depicted by red squares in the graph. Graph shows cumulative distance plots of four vesicles that underwent transport during 60 s (4 d DHC siRNA). Each plot shows the position of the moving vesicle in successive frames relative to the starting position. Black and red plots depict anterogradely and retrogradely moving vesicles, respectively. Both anterogradely transported vesicles and one of the retrogradely moving vesicles (red squares) undergo relatively sustained movement, whereas the other retrogradely moving vesicle spends more time paused than moving. (E) Summary of results of DHC depletion on vesicle transport frequencies and processivity (#test, *, $P < 0.05$). See Results and discussion and Table S1 for details.

In summary, by 2 d after DHC siRNA transfection, when $\sim 35\%$ of the heavy chain is still present, no indication of compromised dynein function is detected by either Golgi distribution or vesicle transport behavior. By 4 d, when the protein level is further diminished to $\sim 20\%$ of control, predictable effects of dynein suppression are apparent. The effects on vesicle transport (although showing some bias in the retrograde direction with regard to the sustained movements) are apparent in both the anterograde and retrograde directions, which is consistent with previous studies indicating that inhibition of either kinesin or cytoplasmic dynein affects both directions of transport (Martin et al., 1999; Gross et al., 2002). The reason for such bidirectional inhibition is unclear, but possibly relates to the mechanisms by which various motors coordinate with one another. The fact that no noticeable changes were apparent at 2 d suggests that 3–4 d is the earliest time point at which dynein levels are sufficiently reduced to reliably produce predictable and specific dynein deficits. Studies on NF transport at 2 d also failed to reveal any deficits (Table S2, available at <http://www.jcb.org/cgi/content/full/jcb.200407191/DC1>), and hence

we focused on 3–4 d as our earliest time point for detailed analyses on deficits in NF and MT transport.

Effects of inhibition of cytoplasmic dynein on NF polymer distribution and transport in the axon

Cytoplasmic dynein has been shown to interact with NF proteins (Wagner et al., 2004) and to move NFs in relation to MTs in vitro (Shah et al., 2000). To investigate effects of dynein depletion on NF transport in axons, we performed the NF transport assay as previously described (Roy et al., 2000; Francis et al., 2005) on neurons exposed to DHC siRNA. The distribution of EGFP-NFH revealed a distal accumulation of NFs in DHC siRNA-treated neurons (Fig. 3, A–D) from day 4 (but not day 2). In controls, we observed fast moving NFs in natural gaps or in photobleached regions in axons, similar to that reported previously (Roy et al., 2000; Wang et al., 2000; Fig. 3 E). These movements occur in both anterograde and retrograde directions, with a frequency ratio of roughly 1:1 (see Table S2 for details). However, in neurons treated with DHC siRNA for 5 to

8 d, the frequency of retrograde movements was dramatically decreased, whereas that of anterograde movements increased (Table S2), resulting in a large increase of the anterograde to retrograde movement ratio ($\sim 24:1$; Fig. 3 F).

The specific inhibition of retrograde transport, which is dissimilar to the effects on MTs (see the following section), is consistent with the cargo model, but inconsistent with the idea of NFs piggy backing on moving MTs. The cargo model also fits well with the results of studies on the transport of intermediate filaments by molecular motors in other systems (Helfand et al., 2002; Xia et al., 2003).

Effects of inhibition of cytoplasmic dynein on MT polymer transport in the axon

To assay MT transport, we used the photobleach method of Wang and Brown (2002), except that we expressed EGFP-tubulin rather than injecting rhodamine-tubulin. We analyzed MT transport behaviors after 4 d of siRNA transfection, by which time the decrease of DHC level had significantly inhibited dynein function, as revealed by Golgi distribution, vesicle transport, and NF transport. In neurons cotransfected with control siRNA, the majority of moving MTs was transported in the anterograde direction, with an anterograde to retrograde frequency ratio of $\sim 2:1$ (see Table S3 for details, available at <http://www.jcb.org/cgi/content/full/jcb.200407191/DC1>). In

DHC siRNA-treated neurons, the frequency of anterograde MT movements is diminished (χ^2 , $P < 0.05$), whereas that in the retrograde direction remains unchanged, resulting in a drop of anterograde to retrograde movement ratio to 1:1 (Table S3). At day 7, a similar decrease is observed in the anterograde frequency, as well as the anterograde to retrograde ratio of MT movements. There is a small diminution in the frequency of retrograde transport of MTs at day 7, but this did not achieve statistical significance (Fig. 4 B). Combining the data from days 4 and 7, the frequency of anterograde MT movements is significantly diminished upon dynein inhibition by RNAi (χ^2 , $P < 0.05$), but the frequency of retrograde MT movements is not significantly affected. Comparing populations of control and DHC-depleted axons, there was no significant difference between the instantaneous velocities (Fig. 4, F and G), but there was a small but statistically significant decrease in the average velocities of both anterograde (2-tailed *t*-test, $P < 0.0001$) and retrograde movements (2-tailed *t*-test, $P < 0.05$; Fig. 4, D and E) in DHC siRNA-treated axons due to a prolongation of the period of time MTs spend in pausing (Table S3).

These results demonstrate that cytoplasmic dynein is a major participant in the anterograde transport of MTs, therefore supporting the sliding filament model for axonal MT transport. We cannot conclude whether or not cytoplasmic dynein is the only motor that fuels the anterograde movements because the neurons

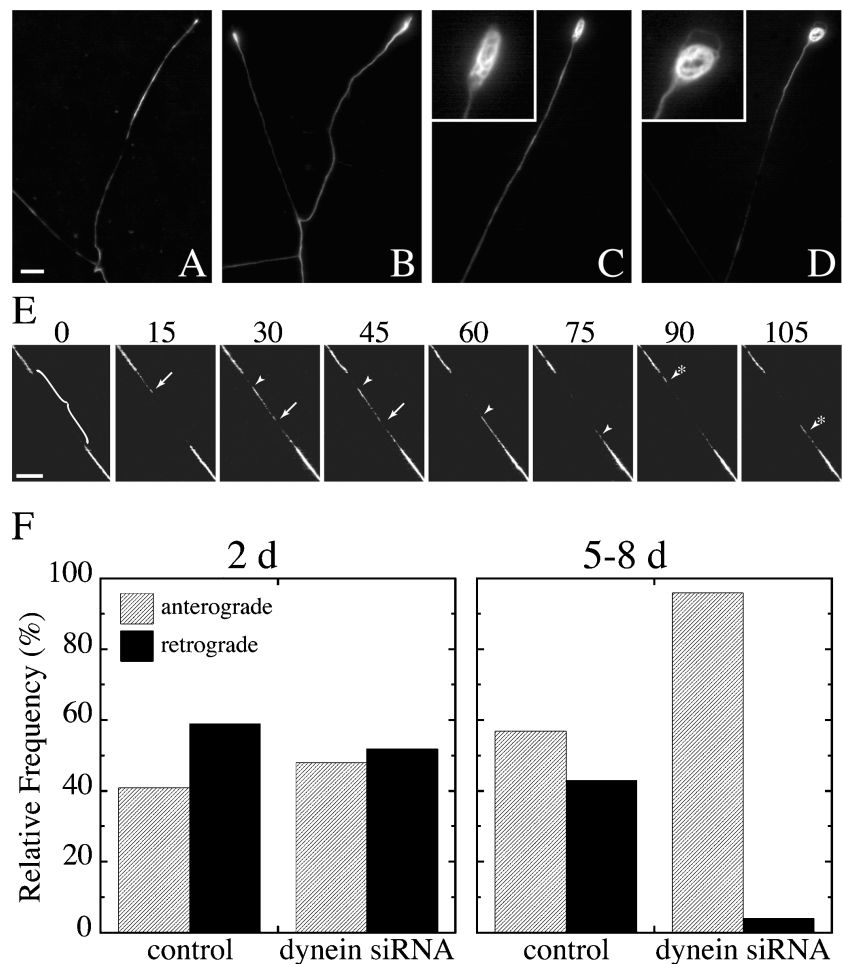


Figure 3. Retrograde NF transport is suppressed in DHC-depleted neurons. A–D show GFP-NFH fluorescence in living neurons treated with control siRNA (A) or DHC siRNA for 4 d (B) or 6 d (C and D). The insets in C and D show the accumulation and disorganization of NFs in the axonal tip at higher magnification. Bars: (A–E) 8 μm ; (insets) 25 μm . (E) Selected frames from a sequence showing anterograde (upper left-to-lower right) translocation of two NFs. Time in seconds is indicated above each frame. The bracket in the 0 s frame identifies a gap in the fluorescent NF array generated by photobleaching. The arrows and arrowheads identify the leading and trailing end, respectively, of a moving NF. The front of this fluorescent NF enters the photobleached gap early in the sequence, and can be seen at 15 s. It continues moving into the gap over the next 15 s, pauses for a while, and then moves out of the gap. Only the trailing end of this NF can be seen at 60 and 75 s. A second, shorter NF enters at 90 s (arrowhead with asterisk) and moves steadily through the gap over the next 20–25 s. (F) Histograms of the frequency of anterograde and retrograde NF movements in neurons treated for the indicated times with control or DHC siRNA.

are not completely depleted of the protein. Another possibility is that a minus-end directed kinesin such as CHO2/HSET contributes to the anterograde transport of MTs, and this would presumably be the result of MTs pushing against one another rather than actin filaments (Sharp et al., 1997). In terms of the retrograde movements, the present data provide almost no evidence that cytoplasmic dynein plays a role. It seems reasonable to surmise that a kinesin-related protein fuels the retrograde transport of MTs. A good candidate may be Eg5, whose inhibition causes rapid bursts in axonal growth, which would be consistent with a diminution in retrograde MT transport (Haque et al., 2004).

Ma et al. (2004) recently proposed a model in which unassembled tubulin is transported in the form of an as yet unidentified organelle. Presumably such an organelle would use a kinesin motor for anterograde and cytoplasmic dynein for retrograde movements. Our observation that depletion of dynein diminishes the anterograde but not the retrograde movements is inconsistent

with this model, and hence supports the contention that the moving structures are indeed short MTs (for review see Hasaka et al., 2004). It is worth noting that unlike vesicle transport, which is impaired in both directions after DHC depletion, the transport of MTs or NFs is impaired in only one direction or the other. This finding may be relevant to the differing mechanisms by which polymer transport and vesicle transport are regulated.

Cytoplasmic dynein has a variety of other roles to play, such as the retrograde transport of growth factors to the nucleus (Heerssen et al., 2004) that could affect the expression of myriad genes, including other motor proteins. Thus, it will be necessary to follow up our results with more acute methods for inhibiting dynein functions and with analyses on the broader effects of suppressing dynein expression on the neuron. Even so, the fact that we obtained such different results on MT and NF transport (and such predictable results on Golgi distribution and vesicle transport) provides confidence

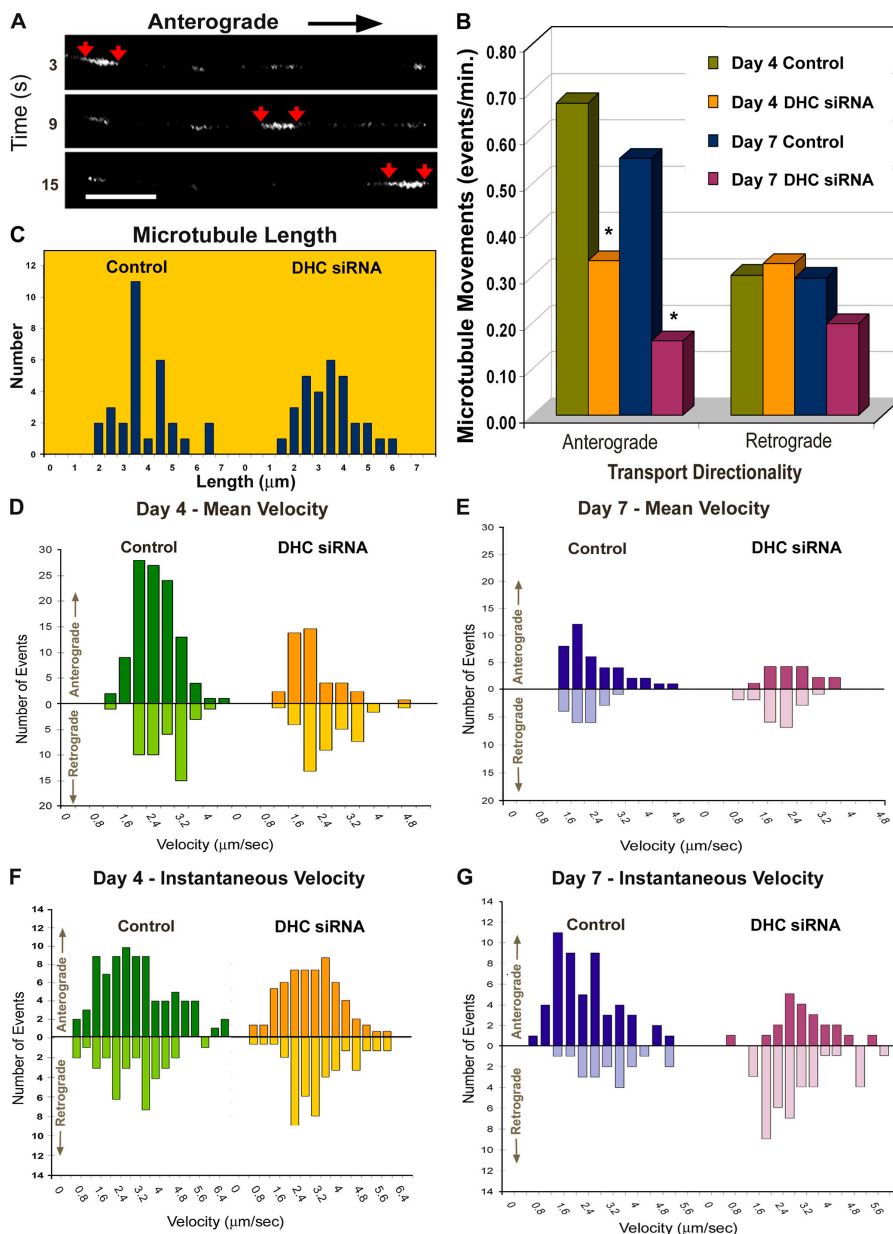


Figure 4. Anterograde MT transport is suppressed in DHC-depleted neurons. (A) Time-lapse images reveal a MT moving in the anterograde direction through the photobleached region. Red arrows mark the leading and trailing ends of the MT. (B) The frequencies (events/min) of anterograde MT transport were significantly decreased in DHC siRNA-treated axons (χ^2 , *, $P < 0.05$) both at 4 and 7 d after siRNA transfection. However, frequencies of retrograde movements were not significantly affected. (C) Histogram showing that there is no significant difference between control and DHC-depleted neurons with regard to lengths of the moving MTs. (D and E) Histograms depict mean velocity distributions of MT movements. (F and G) Histograms depict instantaneous velocity distributions of randomly chosen MTs from the population depicted in D and E, respectively. See Results and discussion and Table S3 for details. Bar, 5 μm.

that our results are specific and not due to a global deficit in neuronal health or viability.

The question arises as to the substrate against which the MTs are transported. We recently reported that pharmacological depletion of actin filaments has very similar effects as those obtained here with depletion of dynein, namely a reduction in the frequency of anterograde but not retrograde MT movements (Hasaka et al., 2004). These results suggest that there may be one category of anterograde MT transport that is both dynein and actin dependent and another category that depends on neither. It is particularly interesting that the axon still grows and the MT array still advances when dynein or actin is depleted, suggesting that the latter category of MT transport may be sufficient to advance the MT array as the axon grows. We suspect that the dynein-driven transport of MTs against actin filaments has unique functions during axonal growth, perhaps to translocate MTs appropriately during guidance of axons to target tissues. Future studies will be aimed at testing this hypothesis, with the goal of assigning particular functions to particular categories of MT transport in the axon.

Materials and methods

Cell culture and transfection

Sympathetic neuronal cultures were prepared and transfected using a nucleofection device (Amaza) as previously described (Hasaka et al., 2004). The EGFP-NFH and EGFP-NFM were obtained and used as previously described (Roy et al., 2000; Wang and Brown, 2002). The EGFP-tubulin construct was purchased from CLONTECH Laboratories, Inc. Four different siRNA duplexes were designed against different regions of the DHC sequence using Dharmacon's custom SMARTpool siRNA service (rat cytoplasmic DHC1; GenBank/EMBL/DDBJ accession no. NM_019226): 5'-gggaggagggtatggttaa-3', 5'-gggtgacagcttcgaatga-3', 5'-ccaatacctacat-tactt-3', and 5'-gctcaaacatgacagaaatt-3'. The nonspecific duplex III (Dharmacon) was used as control. siRNA was dissolved to 200 μ M, aliquoted, and stored at -20°C . siRNA concentration at transfection was 18 μ M.

Immunological techniques

Cultures were fixed in -20°C methanol. Labeling used a polyclonal DHC (R-325) antibody (1:200; Santa Cruz Biotechnology, Inc.) and a monoclonal Golgi-58k antibody (1:500; Sigma-Aldrich). Secondary antibodies were obtained from Molecular Probes and Jackson ImmunoResearch Laboratories (1:200). Images were acquired using equipment previously described (Hasaka et al., 2004) with either a Plan Apochromat 40 \times /1.00 oil objective or a Fluor 100 \times /1.30 oil objective. Fluorescence intensity and surface area were calculated using the "outline" tool within the "measurement" function of Axiovision 4.0.

Western blot analysis

Cultured neuronal lysate was precipitated with cold methanol, dissolved in sample buffer, resolved in 5% SDS PAGE gels, and transferred onto nitrocellulose membranes (1,000 mA; 3 h at 4°C). Transfers were probed for DHC (R-325 antibody at 1:75; secondary HRP at 1:400; Pierce Chemical Co.) and stripped and reprobed for MAP1b as described in Slaughter and Black (2003). Antibody chemiluminescence detection used ECL reagents (Pierce Chemical Co.).

Vesicle transport assay

Rhodamine-dextran (MW \sim 10,000; Sigma-Aldrich) was added into culture medium at 1 mg/ml the night before imaging. 15 min before imaging, cultures were rinsed and replaced with L15 medium supplemented with 5% FCS and oxyrase (1:100; Oxyrase Inc.). Cultures were then sealed with glass coverslips. Image acquisition used the system and methods described previously (Roy et al., 2000). A total of 300 time-lapse images were taken at 200-ms exposure and 400-ms intervals for each axon. Each dish was imaged for no longer than 80 min. 200 sequence frames were analyzed using IP Lab under blinded conditions. Processive movement was defined as movement without reversal of direction or pausing >25 frames.

NF transport assay

Sympathetic neurons cultured in N2 medium (\sim 4 neurons/ mm^2) were treated with laminin (1:400) 24 h after transfection. The EGFP-NFM plasmid was used for imaging on days 2, 3, and 4. Longer treatments used adenovirus carrying EGFP-NFH as described in Roy et al. (2000) and Francis et al. (2005), with the following modifications. Infection was performed on day 2, laminin added on day 3, and images taken on days 5–8. NF transport imaging was performed as described in Roy et al. (2000) and Francis et al. (2005).

MT transport assay

Sympathetic neurons were cotransfected with a tubulin-EGFP plasmid and either DHC siRNA or control siRNA. Cells were cultured for either 4 or 7 d before imaging. EGFP-tubulin-expressing neurons were assayed and analyzed for MT transport as described previously (Hasaka et al., 2004) with either a 900- or 1,200-ms exposure. Recording time ranged from 11 to 15 min (242 to 301 image cycles).

Statistical analyses were performed in Microsoft Excel using $P < 0.05$ as the standard for significant difference.

Online supplemental material

Tables S1, S2, and S3 show data from the vesicle transport assay, the NF transport assay, and the MT transport assay, respectively. Online supplemental material is available at <http://www.jcb.org/cgi/content/full/jcb.200407191/DC1>.

We thank Theresa Slaughter for assistance. We thank Ron Liem for providing tools for NF expression in neurons. We also thank Drs. Scott Brady, Daniel Buster, Irina Tint, Gianluca Gallo, Robert Loudon, Tom Hasaka, Liang Qiang, and Kevin Pfister for advice.

This work was supported by National Institutes of Health grants to P.W. Baas and M.M. Black.

Submitted: 29 July 2004

Accepted: 10 January 2005

References

- Abal, M., M. Piel, V. Bouckson-Castaing, M. Mogensen, J.B. Sibarita, and M. Bornens. 2002. Microtubule release from the centrosome in migrating cells. *J. Cell Biol.* 159:731–737.
- Ahmad, F.J., C.J. Echeverri, R.B. Vallee, and P.W. Baas. 1998. Cytoplasmic dynein and dynactin are required for the transport of microtubules into the axon. *J. Cell Biol.* 140:391–401.
- Black, M.M., and R.J. Lasek. 1980. Slow components of axonal transport: two cytoskeletal networks. *J. Cell Biol.* 86:616–623.
- Bloom, G.S., T.A. Schoenfeld, and R.B. Vallee. 1984. Widespread distribution of the major polypeptide component of MAP 1 (microtubule-associated protein 1) in the nervous system. *J. Cell Biol.* 98:320–330.
- Brady, S.T. 2000. Neurofilaments run sprints not marathons. *Nat. Cell Biol.* 2:E43–E45.
- Dillman, J.F., L.P. Dabney, S. Karki, B.M. Paschal, E.L.F. Holzbaur, and K.K. Pfister. 1996. Functional analysis of dynactin and cytoplasmic dynein in slow axonal transport. *J. Neurosci.* 16:6742–6752.
- Dujardin, D.L., L.E. Barnhart, S.A. Stehman, E.R. Gomes, G.G. Gundersen, and R.B. Vallee. 2003. A role for cytoplasmic dynein and LIS1 in directed cell movement. *J. Cell Biol.* 163:1205–1211.
- Francis, F., S. Roy, S.T. Brady, and M.M. Black. 2005. Transport of neurofilaments in growing axons requires microtubules but not actin filaments. *J. Neurosci. Res.* 79:442–450.
- Gross, S.P., M.A. Welte, S.M. Block, and E.F. Wieschaus. 2002. Coordination of opposite-polarity microtubule motors. *J. Cell Biol.* 156:715–724.
- Haque, S.A., T.P. Hasaka, A.D. Brooks, P.V. Lobanov, and P.W. Baas. 2004. Monastrol, a prototype anti-cancer drug that inhibits a mitotic kinesin, induces rapid bursts of axonal outgrowth from cultured postmitotic neurons. *Cell Motil. Cytoskeleton.* 58:10–16.
- Hasaka, T.P., K.A. Myers, and P.W. Baas. 2004. Role of actin filaments in the axonal transport of microtubules. *J. Neurosci.* 24:11291–11301.
- Heerssen, H.M., M.F. Pazyra, and R.A. Segal. 2004. Dynein motors transport activated Trks to promote survival of target-dependent neurons. *Nat. Neurosci.* 7:596–604.
- Helfand, B.T., A. Mikami, R.B. Vallee, and R.D. Goldman. 2002. A requirement for cytoplasmic dynein and dynactin in intermediate filament network assembly and organization. *J. Cell Biol.* 157:795–806.
- Hollenbeck, P.J. 1993. Products of endocytosis and autophagy are retrieved

- from axons by regulated retrograde organelle transport. *J. Cell Biol.* 121:305–315.
- Lim, S.S., K.J. Edson, P.C. Letourneau, and G.G. Borisy. 1990. A test of microtubule translocation during neurite elongation. *J. Cell Biol.* 111:123–130.
- Ma, Y., D. Shakiryanova, I. Vardya, and S.V. Popov. 2004. Quantitative analysis of microtubule transport in growing nerve processes. *Curr. Biol.* 14:725–730.
- Martin, M., S.J. Iyadurai, A. Gassman, J.G. Gindhart, T.S. Hays, and W.M. Saxton. 1999. Cytoplasmic dynein, the dynactin complex, and kinesin are interdependent and essential for fast axonal transport. *Mol. Biol. Cell.* 10:3717–3728.
- Roy, S., P. Coffee, G. Smith, R.K.H. Liem, S.T. Brady, and M.M. Black. 2000. Neurofilaments are transported rapidly but intermittently in axons: implications for slow axonal transport. *J. Neurosci.* 20:6849–6861.
- Schroer, T.A. 2004. Dynactin. *Annu. Rev. Cell Dev. Biol.* 20:759–779.
- Shah, J.V., L.A. Flanagan, P.A. Janmey, and J.F. Leterrier. 2000. Bidirectional translocation of neurofilaments along microtubules mediated in part by dynein/dynactin. *Mol. Biol. Cell.* 11:3495–3508.
- Sharp, D.J., R. Kuriyama, and P.W. Baas. 1997. Expression of a minus-end-directed motor protein induces Sf9 cells to form axon-like processes with uniform microtubule polarity orientation. *J. Cell Sci.* 110:2373–2380.
- Slaughter, T., and M.M. Black. 2003. STOP (stable-tubule-only-polypeptide) is preferentially associated with the stable domain of axonal microtubules. *J. Neurocytol.* 32:399–413.
- Wagner, O.I., J. Ascano, M. Tokito, J.F. Leterrier, P.A. Janmey, and E.L. Holzbaur. 2004. The interaction of neurofilaments with the microtubule motor cytoplasmic dynein. *Mol. Biol. Cell.* 15:5092–5100.
- Wang, L., and A. Brown. 2001. Rapid intermittent movement of axonal neurofilaments observed by fluorescence photobleaching. *Mol. Biol. Cell.* 12:3257–3267.
- Wang, L., and A. Brown. 2002. Rapid movement of microtubules in axons. *Curr. Biol.* 12:1496–1501.
- Wang, L., C.L. Ho, D. Sun, R.K.H. Liem, and A. Brown. 2000. Rapid movement of axonal neurofilaments interrupted by prolonged pauses. *Nat. Cell Biol.* 2:137–141.
- Xia, C.H., E.A. Roberts, L.S. Her, X. Liu, D.S. Williams, D.W. Cleveland, and L.S. Goldstein. 2003. Abnormal neurofilament transport caused by targeted disruption of neuronal kinesin heavy chain KIF5A. *J. Cell Biol.* 161:55–66.